JOURNAL OF GEOPHYSICAL RESEARCH, VOL. 96, NO. C4, PAGES 7127–7136, APRIL 15, 1991

The Role of the Turbulent Stress Divergence in the Equatorial Pacific Zonal Momentum Balance

D. HEBERT, J. N. MOUM, C. A. PAULSON, AND D. R. CALDWELL

College of Oceanography, Oregon State University, Corvallis

T. K. CHERESKIN

Scripps Institute of Oceanography, University of California, San Diego, La Jolla

M. J. MCPHADEN

Pacific Marine Environmental Laboratory, National Oceanic and Atmospheric Administration, Seattle, Washington

From a comprehensive set of upper ocean measurements made during a moderate El Niño in boreal spring 1987, we reassess the role of turbulence in transporting momentum vertically at the equator. An examination of the terms in the vertically integrated zonal momentum equations indicates that on short time scales the zonal pressure gradient is not balanced by the surface wind stress despite an apparent balance of these terms on longer (seasonal) time scales. The vertical redistribution of zonal momentum is complex. The strength of the wind determines both the magnitude and, likely, the mechanisms of momentum transport between the surface and the core of the undercurrent. During low wind conditions in April 1987 the turbulent stress divergence was significantly different in magnitude and vertical structure from that found during strong winds in November 1984. In November 1984 the turbulent stress divergence was much too large above 40 m to balance the residual term in the zonal momentum budget of Bryden and Brady (1985, 1989) and decayed exponentially with depth from the wind stress value at the surface. In April 1987 the turbulent stress divergence was smaller than that required by Bryden and Brady and decayed linearly from the surface wind stress. For a proper comparison with Bryden and Brady's zonal momentum balance, it is necessary to determine the annual average turbulent stress divergence.

1. INTRODUCTION

The zonal momentum balance in the equatorial Pacific was first investigated by *Sverdrup* [1947], who inferred a balance between the vertically integrated zonal pressure gradient and the zonal wind stress. Apparently, the pressure gradient–wind stress balance holds on the annual (and possibly, seasonal) time scale [*Katz et al.*, 1977; *Tsuchiya*, 1979; *Bryden and Brady*, 1985; *McPhaden and Taft*, 1988]. The other terms in the momentum balance must act to redistribute momentum vertically. Hence we expect a distinct vertical structure to the momentum balance. *Bryden and Brady* [1985, 1989] attempted to determine the importance of the different terms in the momentum balance as a function of depth between 150°W and 110°W. For the annual mean, they found the nonlinear mean advection and eddy flux terms to be important, but a vertical eddy viscosity of $O(10^{-3}$ m^2 s$^{-1})$ for processes smaller than mesoscale eddies was needed to close the budget. Estimates of the turbulent stress divergence at the equator over a 12-day period in November 1984 were found to be too large in the upper 40 m to close the *Bryden and Brady* [1985, 1989] momentum budget [*Dillon et al.*, 1989]. The vertical decay scale of turbulent stress was much smaller than that for the pressure gradient, and the turbulent stresses were too small below 40 m to match the stress required in *Bryden and Brady*'s [1985, 1989] balance.

In this paper we examine some of the terms in the zonal momentum balance using data from an equatorial transect made in April 1987. In section 2 the large-scale structure of the upper ocean in the equatorial Pacific Ocean during boreal spring 1987 is compared with climatological conditions and conditions found in November 1984. During spring 1987 a pulselike disturbance which depressed the thermocline and equatorial undercurrent (EUC) dominated the upper ocean conditions at 140°W. In section 3 we examine the structure of the different terms in the zonal momentum balance. Unlike the success that *Wilson and Leetmaa* [1988] had in determining zonal advection of zonal momentum and the zonal pressure gradient for their equatorial transects and momentum balance, we will show that the effect of the depression of the thermocline and the undercurrent dominates these two terms in our momentum budget. This transient feature does not appear to affect the turbulent stress divergence term. The vertical structure of the turbulent stress found during April 1987 is significantly different from that found in November 1984 by *Dillon et al.* [1989].

2. EQUATORIAL CONDITIONS DURING BOREAL SPRING 1987

The measurements discussed here are a subset of a larger experiment. In March 1987 a transect was made from 33°N to 6°S along 140°W with a 1 day stop at 1°N. Following refueling in Tahiti, a second transect from 140°W to 110°W along the equator was executed, and the experiment ended with a third transect from 3°S to 6°N along 110°W. In this paper, we are interested in the behavior at the equator;

Paper number 91JC00271.
0148-0227/91/91JC-00271$05.00

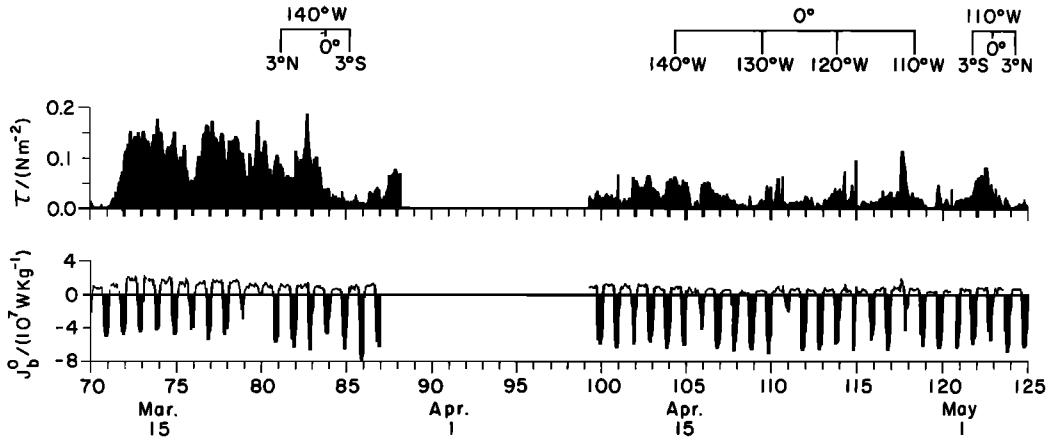

Fig. 1. Wind stress magnitude τ and surface buoyancy flux J_b^0 during the spring 1987 survey. Periods of negative J_b^0 (daytime heating) are shaded. Representative locations along the three transects are shown. Time is in Julian days (representative calendar dates are also shown).

therefore we consider the data from three regions: transect 1, 3°N to 3°S along 140°W (March 22 to March 26); transect 2, 140°W to 110°W along the equator (April 14 to April 28); and transect 3, 3°S to 3°N along 110°W (May 1 to May 4). For convenience, these transects are referred to in the text as T1, T2, and T3.

Vertical profiles of temperature, conductivity, and small-scale shears to a depth of approximately 150 m were obtained approximately every 10 min with the rapid sampling vertical profiler (RSVP) [*Caldwell et al.*, 1985], resulting in a vertical profile approximately every 1.5 km with a typical ship speed of 5 knots (0.51 m s^{-1} Temperature, salinity and other related properties (e.g., σ_t) were averaged vertically over 2 m. Turbulent kinetic energy dissipation rates (ε) were determined from the averaged (2- to 4-m vertical bins) variance from the shear probes [*Osborn and Crawford*, 1980]. Vertical profiles of horizontal currents were obtained every 30 s with a RDI 300-kHz acoustic Doppler current profiler (ADCP). ADCP velocities were screened with a signal-to-noise criterion that corresponded to less than 1 cm s^{-1} noise bias in the screened velocities [*Chereskin et al.*, 1989]. The screening criterion is equivalent to a cutoff depth (164 m) below which velocities were considered unreliable. Horizontal velocity components were determined every 4 m but are independent only over scales greater than 12 m [*Chereskin et al.*, 1986]. From these data, hourly averaged profiles of temperature, salinity, density (σ_t), ε, and horizontal velocities were used for the analysis in this paper.

The winds (Figure 1) were moderately strong before the start of T1 on Julian day 81.0624. (We have used Julian day notation for time in this paper. The integer part of the Julian day is the day number of the year since January 1, 1987, with January 1 as day 1, and the time of day (UT) is given as a fraction of the day. Figure 1 shows the calendar day for several of the Julian days.) The wind stress generally decreased over T1 except for a period of approximately 1 day during which we maintained a 1-day station at 1°N. The average wind stress magnitude during this day (0.09 N m^{-2}) was approximately the same as that found during November 1984 [*Moum et al.*, 1989]. The wind stress was much weaker for the remainder of the experiment. The average wind stress magnitude for T2 was 0.02 N m^{-2}, and for T3, it was 0.03 N m^{-2}. During these transects, there were no strong wind events as found during T1. The direction of the winds was highly variable (i.e., both easterly and westerly winds were observed). By comparison, the winds during the November 1984 experiment at 140°W were from the east and remarkably steady.

The surface buoyancy flux (J_b^0) shows the predominant diurnal cycle (Figure 1) due to daytime heating (negative J_b^0). There was a low-frequency (period of approximately 5 days) variability in the daytime buoyancy flux due to variability in cloud cover. There is evidence of a lower-frequency (approximately 12 days) modulation in the buoyancy flux out of the ocean at night (Figure 1). The magnitudes of the buoyancy flux at night and during the day were similar to those found during November 1984 [*Moum et al.*, 1989; *Peters et al.*, 1989].

During April the surface current at the equator is usually eastward at approximately 0.4 m s^{-1} while in November the velocity is westward at approximately 0.4 m s^{-1} [*McPhaden and Taft*, 1988]. An anomalous situation existed at the equator in April 1987. At 140°W the velocity was weak (<0.2 m s^{-1} for depths less than 40 m) and eastward for T1 (Figure 2). Twenty days later, at the start of T2, the surface current was weak and to the west. As we progressed eastward during T2 the current changed back to eastward and increased in strength, reaching a maximum at approximately 122°W. With weaker westward winds we would expect a stronger eastward current at the surface; other conditions remaining constant. The variability in strength and depth of the EUC plays a role in the variability of the surface current. Normally, the eastward flowing EUC is shallower and stronger in spring than in fall. In spring 1987, the EUC was much weaker than is normally found at this time.

The core of the eastward flowing Pacific equatorial undercurrent was located at a depth of 100 m at 140°W and had a velocity of approximately 1 m s^{-1} (Figure 2). During February–April 1987 the EUC was weaker than the climatological average by 0.25 to 0.5 m s^{-1} [*McPhaden and Hayes*, 1990]. In fact, the core of the EUC was very weak during February 1987: its velocity was only 0.45 m s^{-1}. The depth of the equatorial undercurrent is typically shallowest during March–April and deepest during November [*McPhaden and Taft*, 1988]. Although the depth of the EUC during April 1987 was deeper than is normally found in April [*McPhaden*

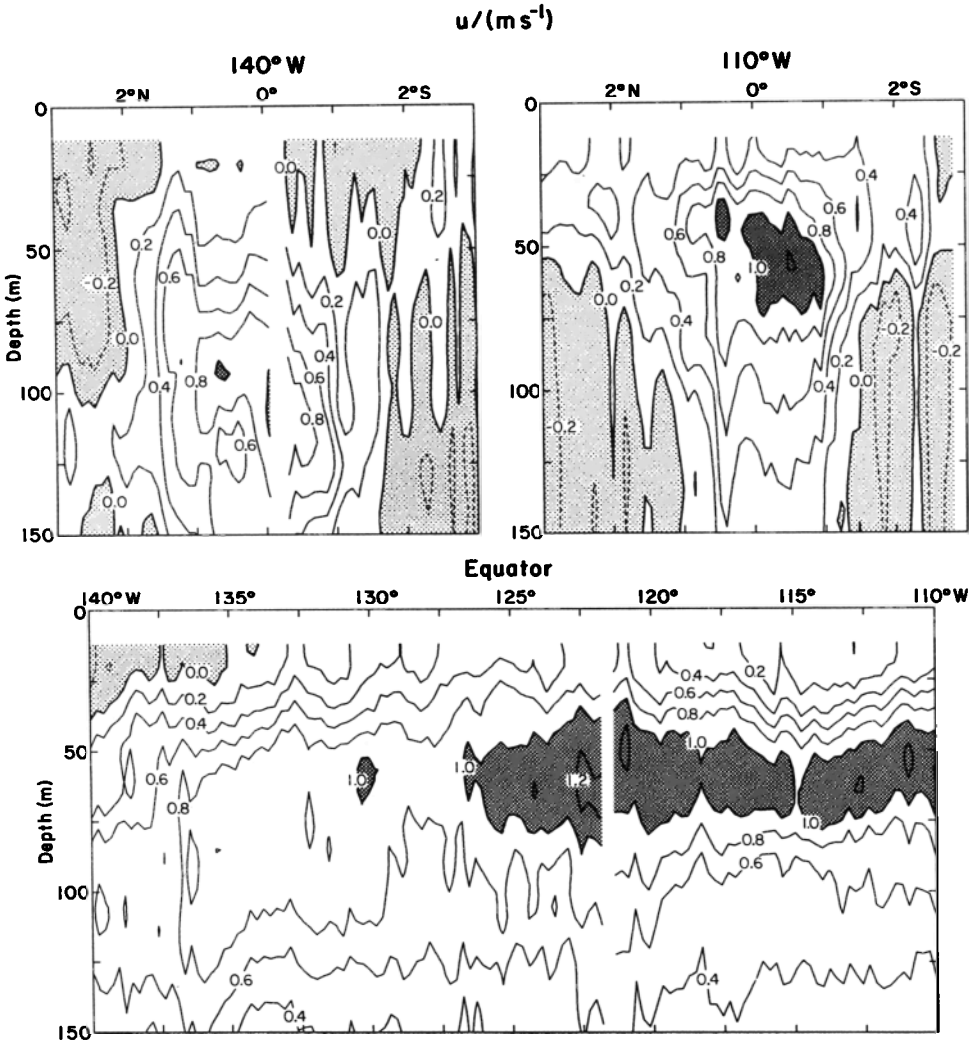

Fig. 2. Eastward velocity structure of the equatorial Pacific for (top left) transect 1 (T1), along 140°W from 3°N to 3°S; (bottom) transect 2 (T2) along the equator from 140°W to 110°W; and (top right) transect 3 (T3), along 110°W from 3°N to 3°S. Contour interval is 0.2 m s^{-1}. Light shading represents regions of westward flow; dark shading represents regions of eastward flow of greater than 1 m s^{-1}.

and Taft, 1988; *Wilson and Leetmaa*, 1988], it was within the interannual variability observed by *McPhaden and Taft* [1988]. The depth and velocity of the EUC at 140°W in April 1987 was more typical of the October–November time period [*Chereskin et al.*, 1986; *McPhaden and Taft*, 1988; *Wilson and Leetmaa*, 1988]. *Bryden and Brady* [1985] found that the annual mean EUC core velocity decreased from 1.27 m s^{-1} at 150°W to 0.98 m s^{-1} at 110°W while it shallowed from 120 m to 60 m. In April 1987 the EUC increased in velocity (to approximately 1.2 m s^{-1}) and shallowed (to a depth of 50 m) between 140°W and 110°W (Figure 2). The structure of the EUC at 110°W during April 1987 was typical of the EUC for April [*Halpern*, 1987; *McPhaden and Taft*, 1988]. As found by *Bryden and Brady* [1985], the EUC was narrower, both horizontally and vertically, at 110°W compared to 140°W. The anomalous conditions found at 140°W were also evident in the density structure.

The density field (Figure 3) in the equatorial region was dominated by temperature except at the surface at 110°W. The low-density water north of the equator (Figure 3) was due to low salinity of the surface water. Low salinity likely arises from net excess precipitation over evaporation associated with the intertropical convergence zone north of the equator [*Bryden and Brady*, 1985]. The pycnocline (and thermocline) generally shallowed from west to east, although the slope is small in spring compared to fall.

Mooring data at the equator show that the thermocline depth varies intraseasonally and seasonally as well as with El Niño events [*Halpern*, 1980; *McPhaden and Taft*, 1988; *McPhaden and Hayes*, 1990]. At 110°W the 20°C isotherm was at approximately 75 m, typical of the normal conditions there. The thermocline at 0°, 140°W for T1 was much deeper than that found 20 days later at the start of T2. The 20°C isotherm rose from 137 m to 92 m over this 20-day period, a change of 45 m. The 20°C isotherm is usually at a depth of 110 m during April, but during an El Niño this isotherm has been found at a depth of 75 m [*Halpern*, 1980; *McPhaden and Taft*, 1988]. Data from a mooring located at 140°W showed that the thermocline depth before day 70 and after day 98 were approximately the same; the 20°C isotherm was at approximately 100 m. Between these days, the thermocline was depressed; the 20°C isotherm reached a depth of

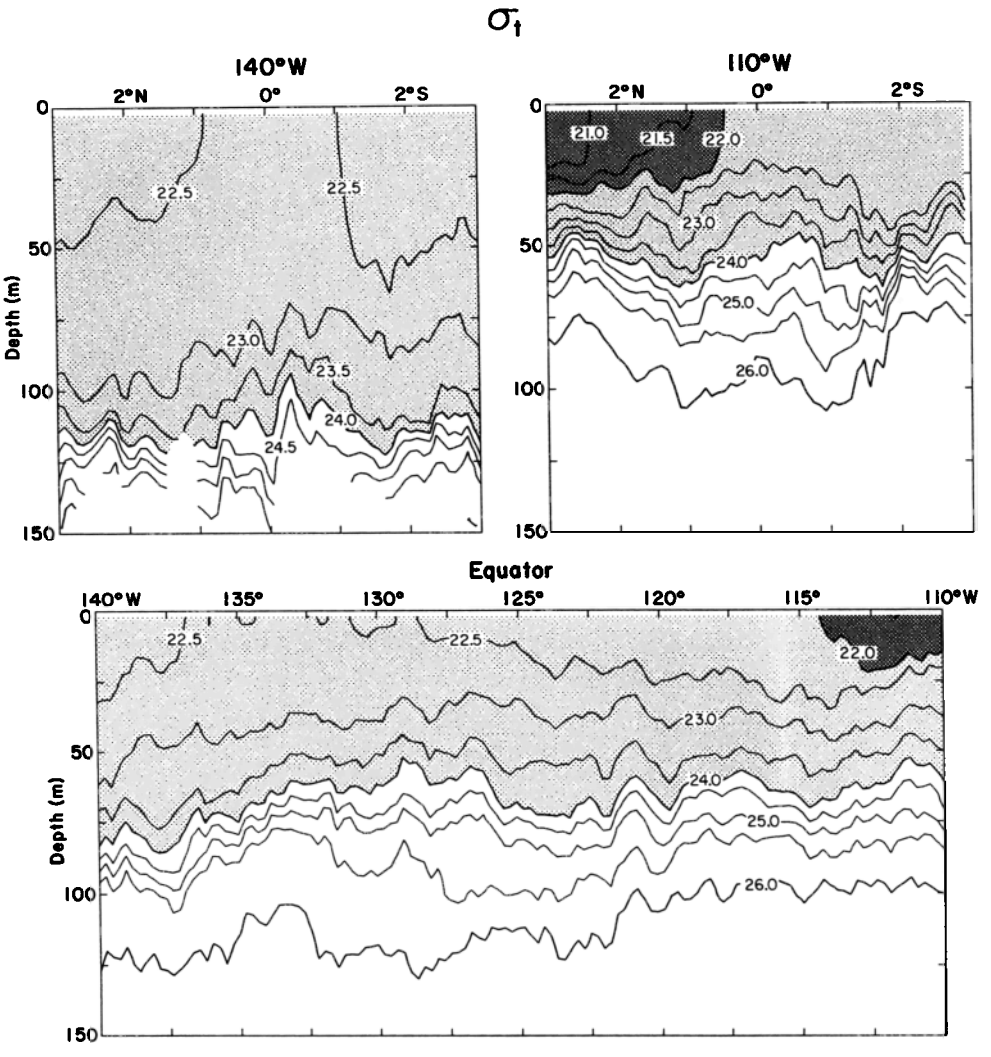

Fig. 3. Density structure (σ_t) of the equatorial Pacific for (top left) T1, along 140°W from 3°N to 3°S; (bottom) T2, along the equator from 140°W to 110°W; and (top right) T3, along 110°W from 3°N to 3°S. Contour interval is 0.5 kg m^{-3}. Light shading represents regions of density less than 24 kg m^{-3}; dark shading represents regions of density less than 22 kg m^{-3}.

approximately 125 m. (With the depth spacing of the temperature sensors on the mooring, it is difficult to determine the depth of isotherms accurately.) West of 130°W during T2 the depth and velocity of the EUC (Figure 2) and the depth of the thermocline changed rapidly. The source of this variability could also have been responsible for the observed change at 140°W between T1 and T2.

Moored velocity, temperature and dynamic height time series from 0, 140°W and 0, 110°W show a pulselike disturbance lasting about 1 month in March–April 1987 [*McPhaden and Hayes*, 1990]. This disturbance propagated eastward at a rate comparable to the phase speed of the first baroclinic mode equatorial Kelvin wave and appeared to have been generated in the western equatorial Pacific by a westerly wind event. Specifically, a 1-month episode of westerlies occurred in February 1987 between about 140°E and the date line with speeds of 5–10 m s^{-1} at and south of the equator [*McPhaden and Hayes*, 1991; *Climate Diagnostics Bulletin*, Climate Analysis Center, NOAA, Washington, D. C., April 1987]. This was followed by a depression of the thermocline, a rise in dynamic height relative to 250 dbar, and increase in eastward transport per unit width between 10 and 250 m in March at 140°W. Similar changes in thermocline depth, dynamic height, and transport were observed beginning about 2 weeks later at 110°W. Longer moored time series records at 140°W and 110°W show that this disturbance was one of several occurring throughout 1986 and 1987, with energy concentrated in spectral bands at periods of approximately 2–3 months as found by *McPhaden and Taft* [1988]. Thus the depression of the thermocline observed in March 1987 during T1 was probably the result of a remotely forced baroclinic Kelvin wave.

The turbulent kinetic energy dissipation rate ε was determined for each of the transects (Figure 4). Although there appears to be no obvious peak in ε in the vicinity of the equator in the cross-equatorial transects at 110°W and 140°W (Figure 4), detailed analysis of the average dissipation rate in the low *Ri* zone below the mixed layer does reveal a peak in ε at the equator (D. N. Hebert et al., Does ocean turbulence peak at the equator?, submitted to *Journal of Physical Oceanography*, 1991, hereinafter referred to as Hebert et al. (1991)). From Figure 4 there is no obvious simple correlation

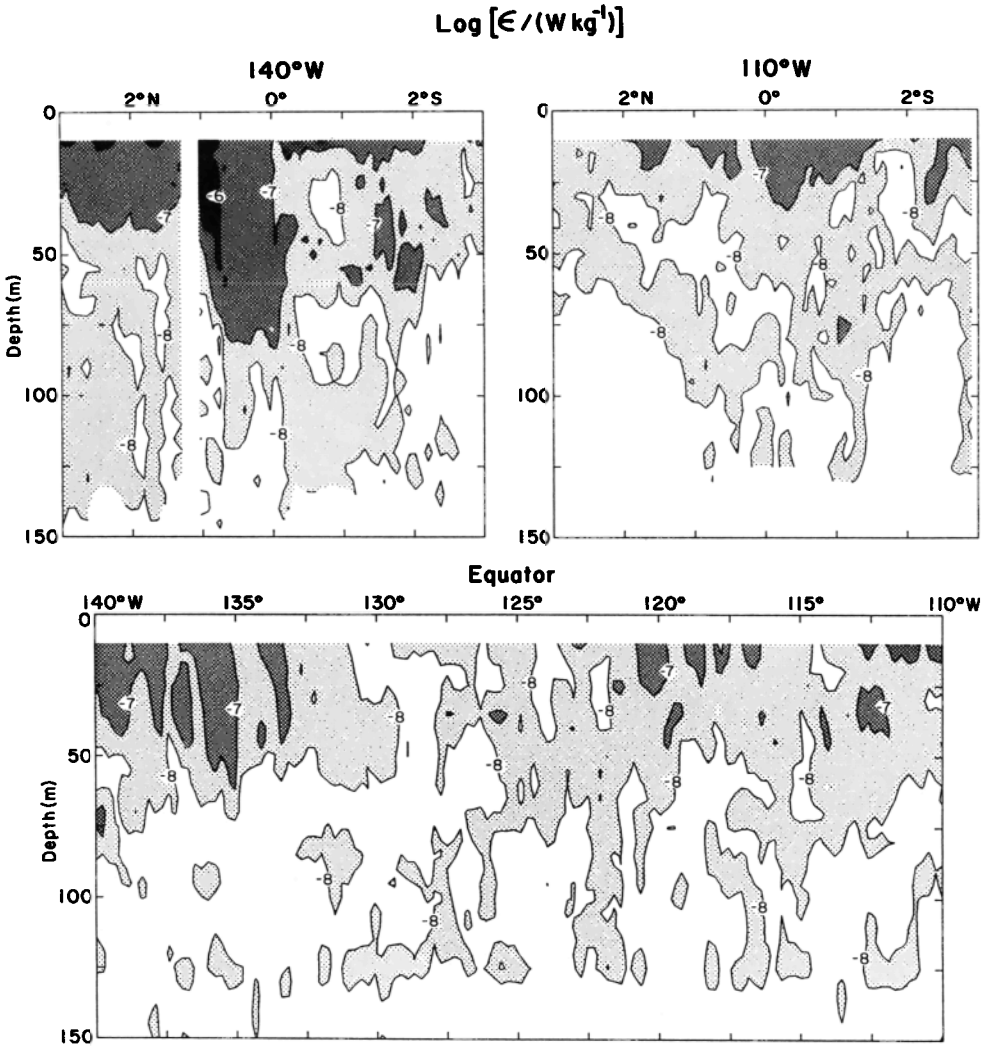

Fig. 4. Turbulent kinetic energy dissipation rate ε of the equatorial Pacific for (top left) T1, along 140°W from 3°N to 3°S; (bottom) T2, along the equator from 140°W to 110°W; and (top right) T3, along 110°W from 3°N to 3°S. Contour interval is 1 decade. Light shading represents regions of ε greater than 10^{-8} W kg^{-1}, darker shading represents regions of ε greater than 10^{-7} W kg^{-1}, and solid shading represents regions of ε greater than 10^{-6} W kg^{-1}.

between ε and the structure of the EUC (e.g., the zonal velocity (Figure 2) of the EUC). Surface forcing (i.e., wind stress) appears to dominate the variability in the dissipation rate in the upper ocean (Hebert et al., 1991). A major surprise in November 1984 was a diurnal cycle in the dissipation rate at 140°W on the equator [*Gregg et al.*, 1985; *Moum and Caldwell*, 1985]. This diurnal cycle was evident between 15 m and 80 m throughout the 12-day experiment in 1984 [*Moum et al.*, 1989]. In 1987 there was a clear diurnal cycle for the first 4 days of T2, when the winds were the strongest. However, the diurnal cycling was neither as strong nor as consistent as was found in 1984 and was not observed during the remainder of T2, with the possible exception of the last 2 days. During the November 1984 survey the winds were significantly larger than those found during T2, and we surmise that the strength of the diurnal signal depends on wind strength. During November 1984 and at the start of T2, large-amplitude, high-frequency internal waves were also observed; the diurnal cycling of ε below the mixed layer is clearly related to these internal waves (J. N. Moum et al., manuscript in preparation, 1991, hereinafter referred to as Moum et al. (1991)).

3. Zonal Momentum Balance

The terms in the zonal momentum equation at the equator have been examined by many authors and by many different methods. Following the success of *Wilson and Leetmaa* [1988] in determining some of the terms from equatorial transects of ADCP, expendable bathythermograph (XBT), and conductivity-temperature-depth (CTD) data, we attempted to determine these momentum terms for T2. We hoped to resolve the discrepancy found by *Dillon et al.* [1989] between the turbulent stress divergence estimate from dissipation measurements made in November 1984 and the expected residual term required to close the zonal momentum budget.

The "mean" zonal momentum equation at the equator can be written as

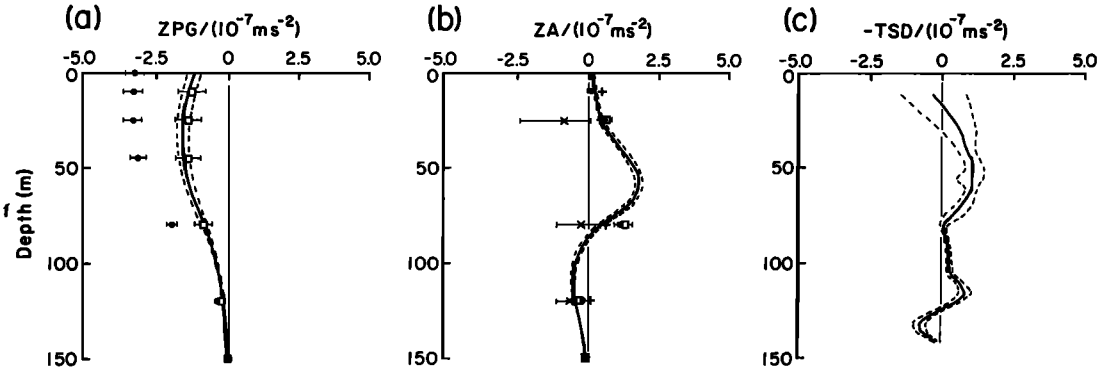

Fig. 5. Average (*a*) zonal pressure gradient (ZPG), (*b*) zonal advection (ZA), and (*c*) turbulent stress divergence (TSD) based on data collected from 140°W to 110°W (transect 2). Dashed lines represent the 95% confidence limits (The 95% confidence limits in Figures 5–8 were determined by the bootstrap method [*Efron and Gong*, 1983]. For bootstrap estimates it is assumed that the data set represents the distribution of the true population. If the decorrelation time and length scales are such that our sample set contained only a few independent realizations of the average pressure field between 140°W and 110°W, the bootstrap confidence limits will underestimate the true confidence limits.) Estimates of the average ZPG and ZA (and 95% confidence limits) based on current meter moorings at 140°W and 110°W for the 15-day period of T2 (open squares) and a 3-month period (solid dots) from March 1 to May 31. LA based on current meter mooring data at 140°W and 110°W for the 15-day period (crosses) and 3-month period (pluses) are shown in Figure 5*b*.

$$\frac{\partial u}{\partial t} + u\frac{\partial u}{\partial x} + v\frac{\partial u}{\partial y} + w\frac{\partial u}{\partial z} + \text{EFD} + \frac{1}{\rho}\frac{\partial p}{\partial x} = \frac{1}{\rho}\frac{\partial \tau^x}{\partial z} \qquad (1)$$

where the velocity components and horizontal gradients have been determined over some suitable time and/or length scale. The averaging time scale and/or length scale is chosen such that motions with times shorter than the averaging time scale or length scale have a zero mean but the correlation between different components of the smaller-scale motion can have a nonzero mean. This is the classical Reynold's decomposition. The eddy flux divergence (EFD) represents scales shorter than the averaging scales but longer than three-dimensional turbulence. We expect that turbulent motions will transport more momentum vertically than horizontally because vertical gradients are much larger than horizontal gradients. Therefore the turbulent stress divergence term TSD (right-hand side) consists of only the vertical component. The other terms in (1) are from left to right, local acceleration (LA), zonal advection (ZA), meridional advection (MA), vertical advection (VA), and zonal pressure gradient (ZPG).

Zonal Pressure Gradient and Zonal Advection

From our April 1987 transect 2 (140°W to 110°W), we obtained velocity data to a depth of 164 m and density and ε to approximately 150 m. As a consequence, we estimated the terms in (1) relative to a depth of 150 m; we note that *McPhaden and Taft* [1988] have shown that most of the variation in the dynamic height field is above 120 m. Zonal gradients (i.e., $\partial p/\partial x$ and $\partial u^2/\partial x$) were estimated from the shipboard transect by linear regression. From the moorings at 140°W and 110°W we estimated ZPG and ZA over the 15-day period of T2. Mean temperature-salinity (T-S) curves at the mooring sites were used to estimate ZPG from the daily-averaged temperature data at the mooring locations. Although the estimates of ZPG and ZA from the spatial transect are subject to temporal aliasing, the spatial variability is well resolved, if the fields were stationary. On the other hand, the mooring estimates of ZPG and ZA provide a well-sampled time series between the two endpoints. The 15-day estimates of ZPG and ZA were compared to estimates over a 3-month period (April–May) from the mooring data.

The dynamic height relative to 150 m showed significant variability on horizontal scales less than 30° of longitude. The depression of the thermocline near 140°W dominated the transect estimate of the mean ZPG between 140°W and 110°W (Figure 5*a*). The mooring estimate of ZPG from the same time period as T2 shows very good agreement with our transect estimate (Figure 5*a*). The 3-month-averaged ZPG (March 1 through May 31) was approximately twice as large as that found during our survey but within range of annual mean ZPG estimates [*Bryden and Brady*, 1985; *McPhaden and Taft*, 1988].

The transect estimate of ZA (Figure 5*b*) shows the eastward increase of eastward velocity above the EUC core and decrease below the core; this trend has been noted by others [e.g., *Bryden and Brady*, 1985; *McPhaden and Taft*, 1988]. As did the dynamic height field, u^2 showed significant variability at many different horizontal length scales from 140°W to 110°W, the depression of the EUC at 140°W dominating the variability. Daily averaged velocities from current meters at 140°W and 110°W showed that estimates of the average ZA for 3 months and 15 days were not significantly different from each other, but they were significantly different from the transect estimates of ZA (Figure 5*b*).

Local Acceleration

LA was estimated from the velocities averaged over the current meters at 140°W and 110°W. Using the daily-averaged current, the mean value of LA for the 15-day and 3-month periods (Figure 5*b*) was small although error bars for the 15-day period were large.

Vertical Advection

From the transect data, it is possible to estimate VA if we assume no mixing and that the flow was along the equator and along isopycnals. That is,

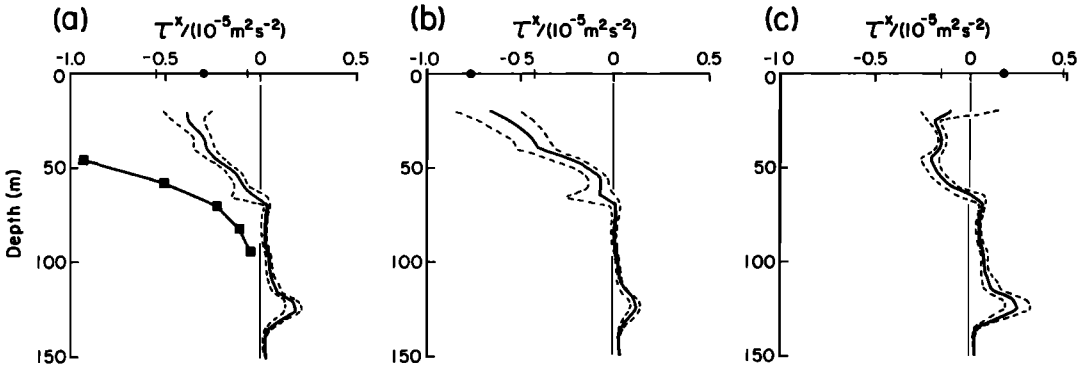

Fig. 6. Average turbulent stress and 95% confidence limits (dashed lines) for T2 data over the longitudinal range (*a*) 140°–110°W, (*b*) 140°–125°W, and (*c*) 125°–110°W. The average zonal wind stress and 95% confidence limits are shown at $z = 0$. The turbulent stress profile from November 1984 is shown by solid squares in Figure 6*a*; the stress estimates above 45 m are off scale.

$$u\frac{\partial \rho}{\partial x} + w\frac{\partial \rho}{\partial z} = 0 \tag{2}$$

Brady and Bryden [1987] found the vertical velocity obtained by assuming the undercurrent flowed along isotherms compared well with estimates based on their diagnostic model [*Bryden and Brady*, 1985]. From (2),

$$\mathrm{VA} = u\frac{g}{\rho N^2}\left(\frac{\partial \rho}{\partial x}\right)\frac{\partial u}{\partial z} \tag{3}$$

This balance breaks down in the mixed layer; it was determined only for depths greater than 20 m. We found the magnitude (not shown) to be much smaller ($<5 \times 10^{-8}$ m s^{-2}) than the other terms calculated. The magnitudes of ZA and VA depend on the slopes of isopycnals. If the flow is along isopycnals, we expect VA to have opposite sign to ZA for the observed conditions (velocity increasing with depth, and isopycnals sloping upward to the east, as above the EUC core). Previous studies [*Bryden and Brady*, 1985; *McPhaden and Taft*, 1988] have found the annual mean value of VA to counteract the annual mean value of ZA, although VA was larger than ZA above the EUC core. For the period of our observations, however, zonal isopycnal gradients were much smaller (Figure 3) than the annual mean; consequently, the flow was more nearly horizontal than the annual mean and VA played an insignificant role.

Turbulent Stress Divergence

Bryden and Brady [1985, 1989] assumed the residual term (LA + ZA + MA + VA + EFD + ZPG) to be the turbulent stress divergence TSD. *Dillon et al.* [1989] used the turbulence measurements collected at 140°W in November 1984 to estimate the turbulent stress divergence term and found that the dissipation estimate of TSD could not account for the residual term of *Bryden and Brady* [1989]. The observed turbulent stress divergence was too large above 50 m and too small below this depth.

The surface value of the turbulent stress is the wind stress, obtained using the bulk formulae of *Large and Pond* [1981]. Within the water column, the turbulent stress was estimated from dissipation and velocity measurements as

$$\tau^x(z) = A_V\frac{\partial u}{\partial z} \qquad A_V = \varepsilon\left[\left(\frac{\partial u}{\partial z}\right)^2 + \left(\frac{\partial v}{\partial z}\right)^2\right]^{-1} \tag{4}$$

The vertical shear was determined over 12 m from hourly ADCP data; ε was averaged over 12 m to match. The method is discussed by *Dillon et al.* [1989]. Divergence of the turbulent stress was determined from the 20 m vertical gradient in the hourly estimates τ^x and averaged over the transect time (Figure 5*c*). It was assumed that the vertical gradient in τ^x at 150 m was zero. In agreement with the November 1984 results [*Dillon et al.*, 1989], we found that when the turbulent stress was extrapolated to the surface it was in reasonable agreement with the wind stress (Figure 6). However, in contrast to the 1984 result, the vertical dependence of the turbulent stress with depth was linear in the upper ocean rather than exponential.

In November 1984 TSD decreased more rapidly with depth than the other annual mean terms in (1). This prompted *Dillon et al.* [1989] to question whether the dissipation method (equation (4)) should be used for estimating A_V or a mechanism other than turbulence is responsible for redistributing momentum vertically. A candidate is the momentum transport by internal gravity waves. During spring 1987, TSD did not show such a rapid decrease with depth (Figure 5*c*); it was much smaller than that found in November 1984 and much smaller than that required to account for *Bryden and Brady*'s [1985, 1989] residual. The most notable difference between 1984 and 1987 observations was the average zonal wind stress; during November 1984 $\tau^x \approx -0.1$ N m^{-2} was approximately 30 times larger than the average zonal wind stress during T2 (Figure 6*a*). Is it possible that this large change in average zonal wind stress might account for the difference in vertical structure of the turbulence stress? During the strongest westward winds (at the start of T2; Figure 1), the turbulent stress was much larger than the transect mean (Figure 6*b*), although it was still 10 times smaller than the average zonal wind stress during November 1984 and still not as large as the value required by *Bryden and Brady* [1985, 1989]. Zonal wind stress and turbulent stress were both weaker for the eastern half of T2 (Figure 6*c*).

The dramatic difference in TSD determined from dissipation measurements in November 1984 and April 1987 sug-

TABLE 1. Depth-Integrated Terms of the Zonal Momentum Equation

	Moorings		Ship			Annual Mean	
	3-Month Average	15-Day Average	140°–110°W	140°–125°W	125°–110°W	*Bryden and Brady* [1985]	*McPhaden and Taft* [1988]
$\int$ ZPG	−28.4 (−31.2, −25.8)	−12.0 (−16.3, −7.9)	−12.9 (−14.5, −11.1)	−26.6 (−31.2, 22.1)	−15.7 (−19.4, −11.6)	−34	−28.7, −49.1
$\int$ LA	3.3 (−1.0, 7.4)	−7.0 (−20.6, −1.5)	...	...	...	...	−2.3, 0.7
$\int$ ZA	7.2 (5.2, 9.2)	8.5 (6.8, 10.2)	6.2 (5.0, 7.8)	15.6 (12.8, 18.3)	−3.8 (−7.3, −0.6)	−0.5	−7.8, −4.9
$\int$ VA	...	...	2.1 (1.3, 2.6)	−3.7 (−5.4, −2.3)	6.2 (4.4, 8.2)	−12.5	−16.1, −17.8
τ^{wind}	−18.7 (−23.8, −14.0)	...	−3.1 (−5.6, −0.8)	−7.7 (−11.0, −4.3)	1.8 (−1.5, 5.0)	−56	−29.5, −55.5

Units are 10^{-6} m^2 s^{-2}. The annual mean results from *Bryden and Brady* [1985] were integrated from the surface to a depth of 500 m. The annual mean results from *McPhaden and Taft* [1988] were integrated from the surface to a depth of 250 m; the left-hand value is the average value over the period November 1983 to November 1984, while the right-hand value is for the period June 1985 to May 1986. The integration range for all of the other integrated terms was from the surface to 150 m. Values in parentheses are the integration of the 95% confidence limits of the momentum terms.

gests that an annual average TSD, which is not known, might account for the TSD required by Bryden and Brady's annual momentum budget above 40 m. It is possible that the November 1984 measurements represent an anomalously large TSD while the April 1987 results are anomalously small. The annual mean TSD would be between these limits and could equal Bryden and Brady's TSD. However, below 40 m the dissipation rates for the November 1984 and April 1987 periods were both too small to produce a TSD large enough to contribute significantly to the momentum budget. It is still necessary to invoke some other small-scale mechanism, such as internal waves, that transport westward momentum from above 40 m to below 40 m (but above the EUC core) to produce the required momentum flux divergence.

Comparison With Annual Means

McPhaden and Taft [1988] found that the annual cycle in the depth-integrated ZPG appeared to be in balance with the annual cycle in wind stress although there were large uncertainties and other processes were likely to be important. We can examine some of the depth-integrated terms in (1) for spring 1987 and compare them with annual mean values. From the moorings at 140°W and 110°W we determined the 15-day (day 104 to day 118) and 3-month (day 60 to day 151) average depth-integrated ZPG, LA, and ZA. Wind data (4 m above sea level) from the mooring at 140°W were available after day 131. At 110°W, good wind velocity data were available from day 70 to day 96 and after day 121. Also, an ATLAS mooring at 125°W gave wind data after day 127. Unfortunately, there were no wind data for the period of T2, and no comparison between wind stress estimates by the anemometers on the moorings to the ship-based stress estimates could be made. A constant-stress, neutrally stable boundary layer was assumed to extrapolate the 4-m winds to 10 m for determination of the zonal wind stress.

For the 3-month average, the depth-integrated ZPG nearly balanced the wind stress, given our large uncertainties (Table 1). Depth-integrated LA and ZA reduced the difference between these two terms. For the 15-day average of the mooring data, the depth-integrated ZPG was approximately half of the 3-month average while the depth-integrated ZA values were approximately the same as the 3-month average. The 15-day average LA was twice as large as the 3-month average LA (although this estimate was not significantly different from zero). Ship-based estimates of these terms (i.e., 140°–110°W averages) agreed with the mooring estimates over the same period. The average zonal wind stress during T2 was less than the typical spring stress (e.g., the 3-month average wind stress). For this period, the wind stress was significantly smaller than the depth-integrated ZPG (Table 1). The difference between the wind stress and depth-integrated ZPG was larger when these terms were estimated over shorter time and space scales (e.g., 140°–125°W and 125°–110°W averages). Waves, such as the Kelvin wave pulse, can greatly affect our estimates of ZPG and ZA over short time periods (Figures 7 and 8).

The April 1987 (day 104 to day 118) depth-integrated momentum terms were quite different from the annual means (Table 1). The depth-integrated values of ZPG and VA were smaller than the annual mean values of *Bryden and Brady* [1985] and *McPhaden and Taft* [1988]. The depth-integrated ZA term for April 1987 was positive, while the annual mean value is negative. This difference is evident from the equatorial velocity structure. In April 1987 the slope of the EUC (Figure 5) was weaker than the annual mean [*Bryden and Brady*, 1985]. Even though the velocity of the EUC was eastward for both cases, the sign and magnitude of $\partial u/\partial x$ is different. For the annual mean structure, this term is negative because the EUC shallows and narrows eastward and its velocity decreases eastward [*Bryden and Brady*, 1985]. In April 1987 the velocity of the EUC increased eastward (Figure 2).

4. SUMMARY AND CONCLUSIONS

During April 1987 the equatorial undercurrent at 140°W was weaker and deeper than normal for this time of year. The strength and depth of the EUC at 110°W was typical of that found during the boreal spring at that location. As the 1987 survey coincided with an El Niño episode, the surface currents and winds were weaker than those normally found in April. A large-scale feature, resulting in the depression of

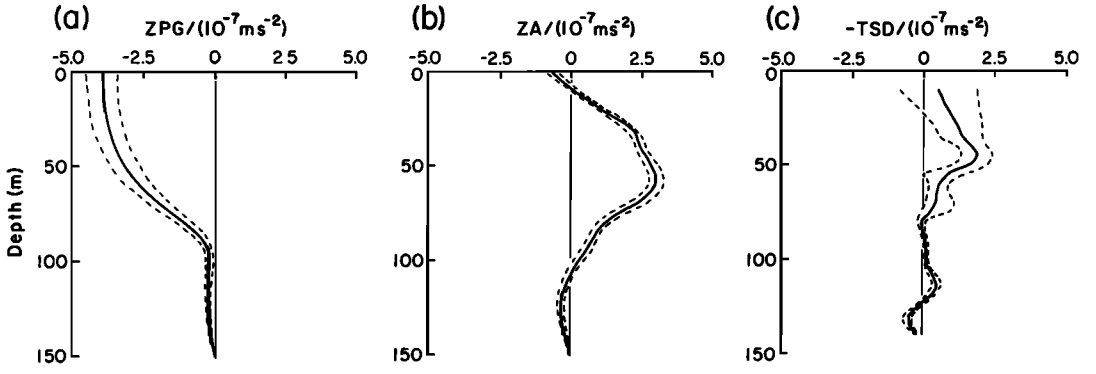

Fig. 7. Average (*a*) ZPG, (*b*) ZA, and (*c*) TSD based on data collected from 140°W to 125°W (western half of T2). Dashed lines represent the 95% confidence limits.

the thermocline and EUC, dominated the western part of the survey region. The depression of the EUC (and the thermocline) from its typical depth occurred before the first transect across the equator at 140°W. At the start of the second survey, 20 days later, the thermocline was returning to its normal springtime depth. On the basis of the data from our equatorial transect and the mooring data from 140°W and 110°W, we believe the disturbance lasted approximately 1 month and propagated eastward at ≈2–3 m s^{-1}. The depression of the EUC was probably due to a Kelvin wave pulse traveling through the region.

The variability in the zonal momentum terms was considerable. From the mooring data at 140°W and 110°W, we found that the average ZPG could change significantly over 15 days: the 3-month average was twice the 15-day average. The transect averaged ZPG (140°W to 110°W) agreed with the mooring ZPG estimate averaged over the same period. During the equatorial transect, the "mean" ZPG over 140°W to 110°W was approximately one quarter to one half of previously annual means [e.g., *Bryden and Brady*, 1985; *McPhaden and Taft*, 1988]; ZA was opposite in sign compared with the annual mean, while VA was much less than the annual mean. The variability in these terms is due to changes in slope and strength of the EUC. Typically, during spring the slope of the EUC is weaker than the annual mean, and ZA is stronger. The 1987 El Niño event must have affected these terms. Shorter period variability (i.e., 60- to 90-day waves) affects estimates of "average" momentum terms when the averaging period is less than the wave period. The "depression" of the thermocline at the start of the 140°–110°W transect significantly changed the structure of ZPG, ZA, and VA. These momentum terms can change over short time and space scales. Single equatorial transects, no matter how densely sampled, can produce an erroneous "mean" of the zonal momentum terms (even if the seasonal average is used as the mean in the zonal momentum balance). Unlike ZPG and ZA, TSD did not appear to be affected by the depression of the EUC and thermocline. Apparently, the variability in wind stress is the controlling factor in the vertical structure of the turbulent stress. For both November 1984 and April 1987, when the turbulent stress estimated by the dissipation method was extrapolated to the surface, it agreed with the estimated zonal wind stress (although for April 1987 the turbulent stress was extrapolated linearly to the surface and for November 1984 it was extrapolated exponentially).

Turbulent stress estimates from November 1984 [*Dillon et al.*, 1989] could not account for the residual term (assumed to be the turbulent stress term) of the annual average momentum balance of *Bryden and Brady* [1985, 1989]. In November 1984, TSD was too large above 40 m and too small below this depth. The turbulent stress term found in April 1987 was smaller than that required by *Bryden and Brady* [1985, 1989] to close the zonal momentum budget at all depths. The vertical structure of TSD in April 1987 was also significantly different from that in November 1984. Below 40 m a mechanism other than three-dimensional turbulence is necessary to account for the stress divergence

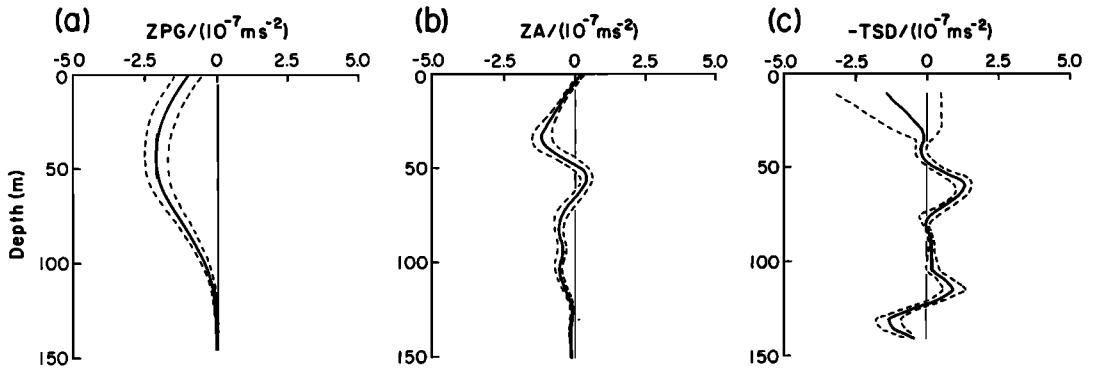

Fig. 8. Average (*a*) ZPG, (*b*) ZA and (*c*) TSD based on data collected from 125°W to 110°W (eastern half of T2). Dashed lines represent the 95% confidence limits.

term of *Bryden and Brady* [1989]. We have observed high-frequency internal waves above the EUC only during periods of high winds (Moum et al., 1991); it is possible that they can redistribute westward momentum vertically [*Wijesekera and Dillon*, 1991]. For a comparison of TSD with the residual term in the *Bryden and Brady* [1985, 1989] momentum budget above 40 m, it will be necessary to determine the annual average component of the turbulent stress signal. The turbulent dissipation data from November 1984 and April 1987 show that variability in the TSD term is large. It seems that it will be necessary to obtain a more extensive set of turbulence measurements over the year to determine the annual average of TSD and that it is this average that should be compared with *Bryden and Brady*'s [1985, 1989] residual term.

In summary, the vertically integrated zonal momentum appears to be a balance between the surface wind stress and zonal pressure gradient on longer than seasonal time scales. For shorter time scales, waves can affect (and dominate) the zonal momentum terms. However, the vertical redistribution of momentum in the upper equatorial ocean is complex. We have now made intensive observations of the upper equatorial ocean during periods of both higher-than-normal and lower-than-normal surface winds. Perhaps a pattern is emerging. Apparently the wind plays an important role in determining both the magnitude and the mechanisms of momentum transport. At low winds, the turbulent stress divergence is relatively small and plays a small role in the local momentum budget. During periods of moderate to high winds, this scenario is radically altered. A large near-surface transport of momentum by turbulence (in which the stress profile is approximately exponential to the surface wind stress) must be balanced by some other mechanism at intermediate depths (but above the EUC core).

Acknowledgments. This work was supported by NSF grant OCE-8716719 and by the Equatorial Pacific Ocean Climate Studies (EPOCS) program.

REFERENCES

Brady, E. C., and H. L. Bryden, Estimating vertical velocity on the equator, *Oceanol. Acta, Spec. Vol. 6*, 33–37, 1987.

Bryden, H. L., and E. C. Brady, Diagnostic model of the three-dimensional circulation in the upper equatorial Pacific Ocean, *J. Phys. Oceanogr., 15*, 1255–1273, 1985.

Bryden, H. L., and E. C. Brady, Eddy momentum and heat fluxes and their effects on the circulation of the equatorial Pacific Ocean, *J. Mar. Res., 47*, 55–79, 1989.

Caldwell, D. R., T. M. Dillon, and J. N. Moum, The rapid sampling vertical profiler—An evaluation, *J. Atmos. Oceanic. Technol., 2*, 615–625, 1985.

Chereskin, T. K., J. N. Moum, P. J. Stabeno, D. R. Caldwell, C. A. Paulson, L. A. Regier, and D. Halpern, Fine-scale variability at 140°W in the equatorial Pacific, *J. Geophys. Res., 91*, 12,887–12,897, 1986.

Chereskin, T. K., E. Firing, and J. A. Gast, Indentifying and screening filter skew and noise bias in acoustic Doppler current profiler measurements, *J. Atmos. Oceanic Technol., 6*, 1040–1054, 1989.

Dillon, T. M., J. N. Moum, T. K. Chereskin, and D. R. Caldwell, Zonal momentum balance at the equator, *J. Phys. Oceanogr., 19*, 561–570, 1989.

Efron, B., and G. Gong, A leisurely look at the bootstrap, the jackknife, and cross-validation, *Am. Stat., 37*, 36–48, 1983.

Gregg, M. C., H. Peters, J. C. Wesson, N. S. Oakey, and T. S. Shay, Intensive measurements of turbulence and shear in the equatorial undercurrent, *Nature, 318*, 140–144, 1985.

Halpern, D., A Pacific equatorial temperature section from 170°E to 110°W during winter and spring 1979, *Deep Sea Res., Part A, 27*, 931–940, 1980.

Halpern, D., Observations of annual and El Niño thermal and flow variations, at 0°, 110°W and 0°, 95°W during 1980–1985, *J. Geophys. Res., 92*, 8197–8212, 1987.

Katz, E. J., R. Belevich, J. Bruce, J. Cochrane, W. Duing, P. Hisard, H. U. Lass, J. Meinke, A. de Mesquita, L. Miller, and A. Rybnikov, Zonal pressure gradient along the equatorial Atlantic, *J. Mar. Res., 35*, 293–307, 1977.

Large, W. G., and S. Pond, Open ocean momentum flux measurements in moderate to strong winds, *J. Phys. Oceanogr., 11*, 324–336, 1981.

McPhaden, M. J., and S. P. Hayes, Variability in the eastern equatorial Pacific during 1986–1988, *J. Geophys. Res., 95*, 13,195–13,208, 1990.

McPhaden, M. J., and S. P. Hayes, On the variability of winds, sea surface temperature and surface layer heat content in the western equatorial Pacific, *J. Geophys. Res., 96*, 3331–3342, 1991.

McPhaden, M. J., and B. A. Taft, Dynamics of seasonal and intraseasonal variability in the eastern equatorial Pacific, *J. Phys. Oceanogr., 18*, 1713–1732, 1988.

Moum, J. N., and D. R. Caldwell, Local influences on shear-flow turbulence in the equatorial ocean, *Science, 230*, 315–316, 1985.

Moum, J. N., D. R. Caldwell, and C. A. Paulson, Mixing in the equatorial surface layer and thermocline, *J. Geophys. Res., 94*, 2005–2021, 1989.

Osborn, T. R., and W. R. Crawford, An airfoil probe for measuring turbulent velocity fluctuations in water, in *Air-Sea Interaction*, edited by F. Dobson, L. Hasse, and R. Davis, pp. 369–386, Plenum, New York, 1980.

Peters, H., M. C. Gregg, and J. M. Toole, Meridional variability of turbulence through the equatorial undercurrent, *J. Geophys. Res., 94*, 18,003–18,010, 1989.

Sverdrup, S. U., Wind-driven currents in a baroclinic ocean with application to the equatorial currents of the eastern Pacific, *Proc. Natl. Acad. Sci., 33*, 318–326, 1947.

Tsuchiya, M., Seasonal variation of the equatorial zonal geopotential gradient in the eastern Pacific Ocean, *J. Mar. Res., 37*, 399–407, 1979.

Wijesekera, H. W., and T. M. Dillon, Internal waves and mixing in the upper equatorial Pacific Ocean, *J. Geophys. Res., 96*, 7115–7125, 1991.

Wilson, D., and A. Leetmaa, Acoustic Doppler current profiling in the equatorial Pacific in 1984, *J. Geophys. Res., 93*, 13,947–13,966, 1988.

D. R. Caldwell, D. Hebert, J. N. Moum, and C. A. Paulson, College of Oceanography, Oregon State University, Corvallis, OR 97331.

T. K. Chereskin, Scripps Institution of Oceanography, University of California, San Diego, La Jolla, CA 92093.

M. J. McPhaden, Pacific Marine Environmental Laboratory, National Oceanic and Atmospheric Administration, 7600 Sand Point Way, NE, Seattle, WA 98115.

(Received March 1, 1990;
revised December 7, 1990;
accepted December 18, 1990.)